# σ-Donor versus $\eta^6$-π-Arene Interactions in Monomeric Europium(II) and Ytterbium(II) Thiolates − An Experimental and Computational Study

**Mark Niemeyer**[a]

*Dedicated to Professor Glen B. Deacon on the occasion of his 65th birthday*

**Keywords:** Ab initio calculations / Lanthanides / π interactions / S ligands / Ytterbium

The base-free, hydrocarbon-soluble complexes $M(SAr^*)_2$ (**4a**: M = Eu, orange; **4b**: M = Yb, purple; $Ar^*$ = 2,6-$Trip_2C_6H_3$; Trip = 2,4,6-$i$$Pr_3C_6H_2$) have been prepared by a protolysis reaction of the Grignard-analogous compound RLnI (R = 2-$F_3CC_6H_4$) with $HSAr^*$. Compound **4b** has been characterized by melting point, elemental analysis, $^1H$, $^{13}C$, and $^{171}Yb$ NMR, IR spectroscopy, UV/Vis spectrophotometry, mass spectrometry, and X-ray crystallography. Additionally, the purple $Yb^{III}$ complex $YbI_2(SAr^*)(THF)_3$ (**3**) and the yellow DME adduct $Yb(SAr^*)_2(dme)_2$ (**5**) have been synthesized and characterized by X-ray crystallography. The solid-state structures of **4a** and **4b** (as THF or benzene hemisolvates) show monomeric units with the metal atom bonded to two terminal thiolate ligands [av. M–S: 281.7 pm (**4a**)/269.1 pm (**4b**)]. Additional $\eta^6$-π-arene interactions are observed to two $C_6H_2$ rings of the Trip substituents [av. M···C: 306.5 pm (**4a**)/297.3 pm (**4b**)]. The binding energy for these interactions has been determined by variable-temperature $^1H$ NMR spectroscopy to be 54.3 kJ $mol^{-1}$ (in methylcyclohexane) and 57.1 kJ $mol^{-1}$ (in toluene). The nature and strength of the $\eta^6$-π-arene bonding has been studied by ab initio calculations on the model systems $[M(arene)]^{2+}$ (arene = $C_6H_6$, $C_6F_6$, 1,3,5-$Me_3C_6H_3$, 1,3,5-$i$$Pr_3C_6H_3$) and $Yb(SH)_2(C_6H_6)_n$ ($n$ = 1, 2). The results are compared with the binding energies in the σ-donor adducts $[M(THF)]^{2+}$, $[M(dme)]^{2+}$, and [M(imidazol-2-ylidene)]$^{2+}$.

## Introduction

The use of charged π-donor ligands and the principle of steric saturation by associated neutral σ-donors or the addition of anionic ligands have dominated organolanthanoid[1] chemistry over the past decades. More recently, however, there has been a growing interest in low-coordinate σ-bonded lanthanoid complexes with bulky substituted organyls,[2,3] Group 14, Group 15, or Group 16 heteroelements.[4] Moreover, the avoidance of coordinating solvents often leads to novel structures and unusual lanthanoid−ligand interactions. Examples of the latter include agostic-type interactions[5] with alkyl-substituted ligands[6−11] or metal−π-arene interactions[12−15] in aryl-substituted ligand systems. In this paper, the synthesis and characterization of the $m$-terphenyl-based[16] metal thiolates $YbI_2(SAr^*)(THF)_3$ (**3**) ($Ar^*$ = 2,6-$Trip_2C_6H_3$; Trip = 2,4,6-$i$$Pr_3C_6H_2$), $M(SAr^*)_2$ [M = Eu (**4a**), Yb (**4b**)], and $Yb(SAr^*)_2(dme)_2$ (**5**) are described. The σ-donor-free compounds **4a** and **4b** show two metal−$\eta^6$-π-arene interactions in the solid state. According to NMR-spectroscopic results, these interactions persist in solution. The nature and strength of these interactions has been studied by ab initio calculations on simple model systems.

[a] Institut für Anorganische Chemie der Universität Stuttgart, Pfaffenwaldring 55, 70569 Stuttgart, Germany
Fax: (internat.) + 49-(0)711/685-4241
E-mail: niemeyer@iac.uni-stuttgart.de

## Results and Discussion

### Syntheses

The syntheses of compounds **1**−**5** are summarized in Scheme 1. Initially, the ytterbium(II) thiolate **4b** was obtained from the reaction of $Yb[N(SiMe_3)_2]_2$ with HSAr*. Mixing the two compounds in $n$-pentane resulted in a color change from orange to purple. Removal of the solvent followed by recrystallization of the residue from a mixture of $n$-heptane and benzene gave **4b** as an extremely air-sensitive crystalline material. However, a much easier route to **4b**, which circumvents the somewhat cumbersome preparation[17] of donor-free $Yb[N(SiMe_3)_2]_2$, is a direct synthesis starting from ytterbium metal and 2-iodobenzotrifluoride. The reaction of lanthanide metals with organyl iodides to give Grignard-analogous compounds RLnI (Ln = Sm, Eu, Yb) has been known for some time.[18] The isolation and structural characterization of such compounds has, however, only recently been achieved.[15,19−21] The initially formed arylytterbium(II) iodide **1b** is instantly protolysed by the thiol HSAr* to give the mixed (thiolato)ytterbium(II) iodide **2b**. Replacing THF by $n$-pentane as the solvent causes the precipitation of $YbI_2(THF)_4$.[22] After removal of the solvent and recrystallization of the residue from an $n$-heptane/toluene mixture, purple **4b** is obtained in 66% yield. The preparation of the donor-free europium(II) thiolate $Eu(SAr^*)_2$ **4a** was accomplished in a similar manner. Attempts to isolate the intermediate mixed (thiolato)-lanthanide(II) iodides **2a** and **2b** did not prove to be successful. Thus, in the case of the ytterbium derivative, crystalliza-

 © WILEY-VCH Verlag GmbH, 69451 Weinheim, 2001 1434−1948/01/0808−1969 $ 17.50+.50/0 

tion at −15 °C only afforded $YbI_2(THF)_4$. Nevertheless, the formation of **2b** was confirmed by its $^{171}$Yb NMR signal. Moreover, it was possible to synthesize the diiodo(thiolato)ytterbium(III) complex **3** in good yield by oxidation of **2b** with iodine. A remarkable feature of the preparation of **4a** and **4b** is the ease with which the coordinated tetrahydrofuran can be removed. Although in the case of **4b** coordination of THF is observed at low temperatures (vide infra), it can be completely removed by pumping at $10^{-3}$ mbar at ambient temperature. In the case of the europium compound, it is even possible to crystallize donor-free **4a** from an *n*-heptane/THF mixture to give the packing complex **4a**·$(THF)_{0.5}$, in which no Eu−O(THF) interactions are observed. This unusual behavior is in contrast to the preparation of other unsolvated lanthanide(II) compounds, e.g. $LnCp^*_2$ or $Ln(OAr)_2$, from solvated complexes, which normally requires repeated sublimation at elevated temperatures.[23] Using dimethoxyethane as a more strongly chelating ligand, it is possible to synthesize the more stable yellow complex $Yb(SAr^*)_2(dme)_2$ (**5**). Even in this case, complete removal of the coordinated solvent can be achieved by pumping overnight at 20 °C/$10^{-3}$ mbar.

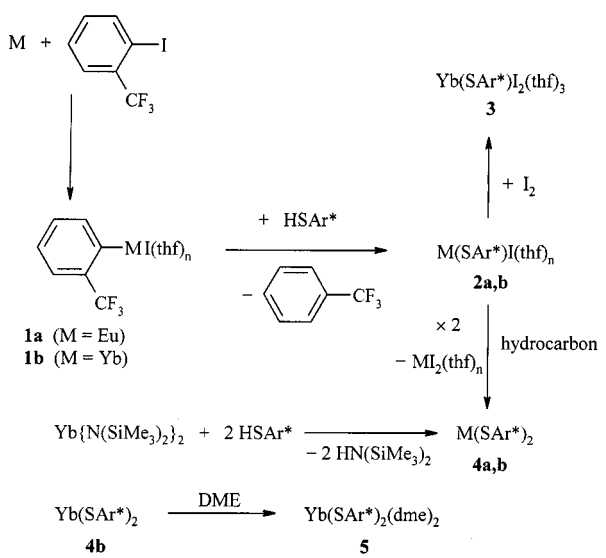


Scheme 1. Syntheses of compounds **1**−**5**

The protolysis of the aryllanthanide(II) iodides **1a** and **1b** seems to be of general interest for the preparation of other lanthanide(II) complexes. In contrast, the usual metathesis reactions often lead to alkali metal halide contaminated products or to the formation of unwanted ate complexes, while the related one-pot transmetallation/protolysis route of Deacon et al.[17] relies on poisonous $Ph_2Hg$. Using our method, we were able to synthesize the known compounds[23] $Yb[N(SiMe_3)_2]_2(THF)_2$, $Yb(OAr')_2(THF)_2$ ($Ar'$ = 2,6-$t$Bu$_2$-4-Me$C_6H_2$), and $YbCp^*_2(THF)_2$ in pure form and good yields.[24] Although the 2-iodobenzotrifluoride used here can be replaced by other aryl iodides, we have found it to be superior, giving shorter reaction times and improved purity of the products.[24]

## X-ray Crystal Structures

Compounds **3**, **4a**, **4b**, and **5** were examined by X-ray crystallography. Their molecular structures are shown in Figures 1, 2, 3 and 4, while salient structural parameters are given in Tables 1, 2 and 3. The solid-state structure of purple $YbI_2(SAr^*)(THF)_3$ (**3**) consists of monomeric units (Figure 1). The central Yb atom shows a distorted octahedral coordination with two iodo ligands in apical positions [I(1)−Yb−I(2) = 176.74(3)°]. Despite the presence of the sterically crowded SAr* ligand, the Yb−S bond length of 258.1(2) pm seems to be the shortest ytterbium−sulfur distance yet reported for a molecular ytterbium compound.[4] It may be compared with the average Yb−S bond lengths in the six-coordinate complexes $Yb(STrip)_3(py)_3$ and *mer*-$Yb(SPh)_3(py)_3$, which were determined as 264.8 pm and 264.7 pm, respectively (Table 4). The shortest Yb−S distance of 260.9(4) pm is found *trans* to one pyridine ligand in the latter. In **3**, the Yb−I bond lengths of 291.0(1) pm [Yb−I(1)] and 298.4(1) pm [Yb−I(2)] are close to the values seen in the previously reported dimeric complex [(μ-OMe)$YbI_2$(dme)]$_2$ (av. 293.2 pm)[25] and the formally eight-coordinate compound $Yb(Cp)_2I(THF)$ (293.2 pm).[26] The different Yb−I bond lengths in **3** can be attributed to the significant deviation of the Yb atom from the S−O(41)−O(51)−O(61) plane by 10.6 pm (Table 1). A notable feature of the structure of **3** is that the Yb−O distances to the coordinated THF ligands are rather different. With a value of 239.0(6) pm, the Yb−O(41) bond *trans* to the SAr* group is unusually long, whereas the others (av. Yb−O = 227.3 pm) are in the normal range for $Yb^{III}$ complexes with six-coordinate metal centers.[27] The long Yb−O(41) bond may be compared with the average Yb−O distance of 239.5 pm *trans* to the $C_6H_5$ groups in *fac*-$YbPh_3(THF)_3$.[28] The *trans* influence of THF ligands in lanthanoid(III) chemistry has been noted previously.[29]

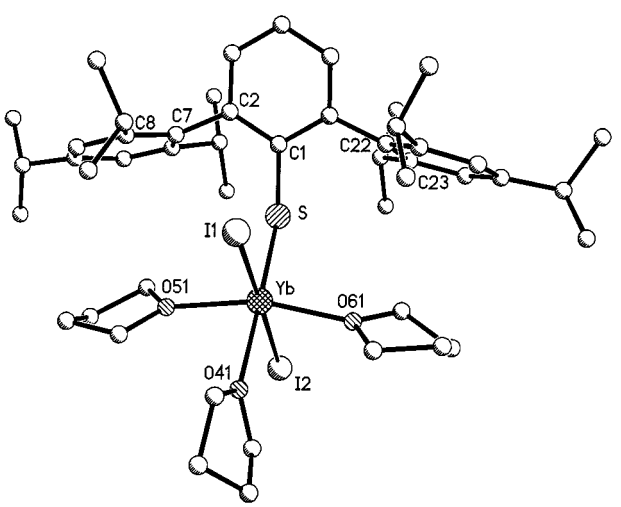


Figure 1. Molecular structure of **3**, showing the atom numbering scheme; hydrogen atoms have been omitted for clarity

Because of their very similar features, the solid-state structures of the compounds $Eu(SAr^*)_2$ [**4a**·$(THF)_{0.5}$] and $Yb(SAr^*)_2$ [**4b**·$(C_6H_6)_{0.5}$] will be discussed together. Both complexes crystallize as monomers. Their molecular struc-

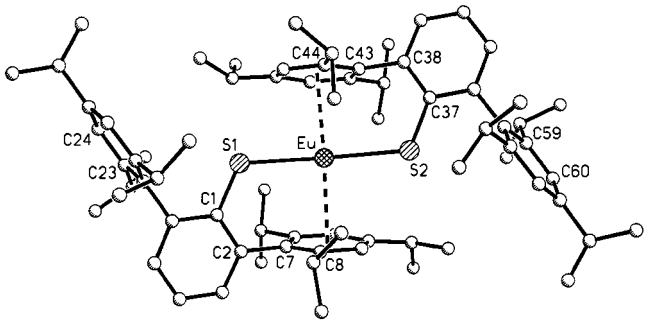


Figure 2. Molecular structure of **4a**, showing the atom numbering scheme for **4a** and **4b**; hydrogen atoms, the minor parts of the disordered isopropyl groups, and the co-crystallized THF molecule have been omitted for clarity

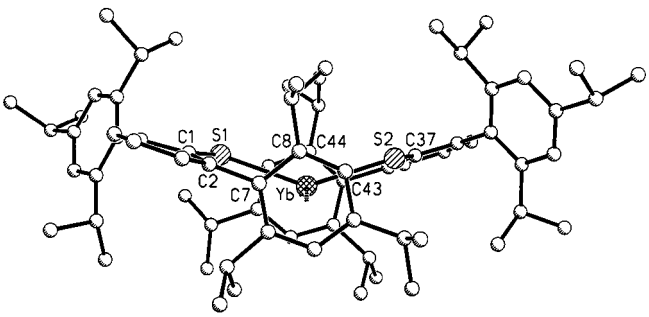


Figure 3. Molecular structure of **4b**, showing the two $\eta^6$-coordinated arene rings and part of the atom numbering scheme; hydrogen atoms, the minor parts of the disordered isopropyl groups, and the co-crystallized benzene molecule have been omitted for clarity

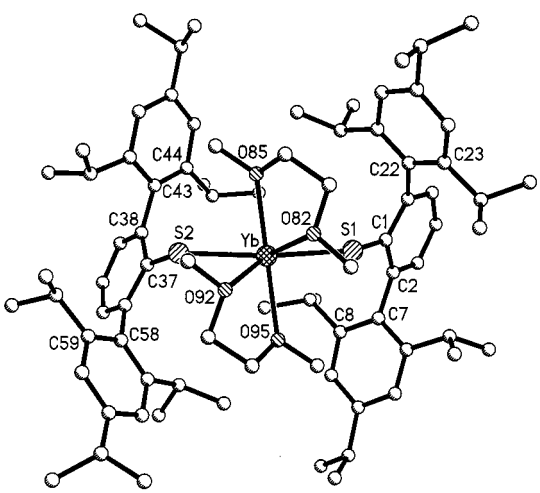


Figure 4. Molecular structure of **5**, showing the atom numbering scheme; hydrogen atoms and the minor parts of the disordered isopropyl groups have been omitted for clarity

tures are illustrated in Figure 2 (**4a**) and Figure 3 (**4b**), while salient bond parameters are listed in Table 2. Despite the difference in the ionic radii of europium(II) and ytterbium(II), both complexes crystallize in isomorphous cells. They differ in the type of solvent that is packed in the cavities of the structure. There are, however, no significant interactions between the metal centers and the co-crystallized tetrahydrofuran or benzene molecules. Each metal atom is coordinated to the sulfur atoms of the thiolate ligands with S−M−S angles of 141.89(4)° (**4a**) and 142.73(8)° (**4b**), respectively. The most striking structural features of **4a** and **4b** are the additional $\eta^6$-π-interactions to two *ortho*-2,4,6-triisopropylphenyl rings of the terphenyl groups (Figure 3). Although the occurrence of two $\eta^6$-π-bonded arene rings is unprecedented for structurally authenticated di- or trivalent lanthanide species,[12] such interactions are well-known in some bis(arene)lanthanide(0) derivatives. Structurally characterized examples include the compounds $M(\eta^6\text{-}1,3,5\text{-}t\mathrm{Bu}_3\mathrm{C}_6\mathrm{H}_3)_2$ (M = Y, Gd, Ho).[30] It should be noted that the cyclometallated scandium(II) complex $\mathrm{ScH}(\eta^6\text{-}t\mathrm{Bu}_3\mathrm{C}_6\mathrm{H}_3)[\eta^6,\eta^1\text{-}(\mathrm{CH}_2\mathrm{CMe}_2)t\mathrm{Bu}_2\mathrm{C}_6\mathrm{H}_3]$, which was formed by C−H insertion from $\mathrm{Sc}(\eta^6\text{-}1,3,5\text{-}t\mathrm{Bu}_3\mathrm{C}_6\mathrm{H}_3)_2$, may also possess two metal−π-arene interactions, although this was based purely on ESR evidence.[31]

The two terphenylthiolate ligands in **4a** and **4b** are orientated in such a way that the most favorable $\eta^6$-π-arene bonding is maximized. In effect, the interplanar angles between the M−S−C planes and the central 2,6-substituted phenyl rings, i.e. A/D and E/H (Table 2), are in the range 0.3° to 6.7°. Together with the perpendicular arrangement of the *ortho*-Trip groups (A/B, A/C, E/F, E/G = 82.0−89.5°), an almost parallel orientation of the C(7)−C(12) and C(43)−C(48) rings to the central S(1)−M−S(2) plane is achieved (B/I, F/I = 6.3−13.6°). Despite the formal coordination number of eight, the observed europium−sulfur and ytterbium−sulfur distances are surprisingly short. In fact, they are ca. 8−13 pm (**4a**) and 7−19 pm (**4b**) pm shorter than the metal−sulfur distances reported for other europium(II) and ytterbium(II) thiolates (Table 4). In **4a**, the europium ion interacts essentially equally with both Trip rings with Eu−C distances in the relatively narrow range of 298.8(3)−315.0(3) pm for C(7)−C(12) and 296.7(3)−316.1(3) pm for C(43)−C(48), with average values of 307.0 pm and 305.9 pm, respectively. In **4b**, the Yb−C interactions to the C(7)−C(12) ring were found to have distances between 287.0(8) and 305.2(8) pm (av. 296.3 pm), with a somewhat greater variation of 282.4(8)−313.9(8) pm (av. 298.3) for the bonding to the second C(43)−C(48) arene ring. The average metal−centroid distances are 272.8 pm (**4a**) and 263.7 pm (**4b**), whereas the X(1)−M−X(2) angles, where X(1) and X(2) define the centroids of the coordinated arene rings, are 166.9° and 164.5° respectively. Salient structural parameters in known compounds with europium− and ytterbium−$\eta^6$-π-arene coordination are summarized in Table 5. The Yb−C interactions in **4b** are comparable to the reported average $Yb^{II}$−C distances, which fall in the range 296−304 pm. In accordance with the smaller radius of $Yb^{III}$, the complex $Yb(C_6Me_6)(AlCl_4)_3$ shows shorter Yb−C distances of 286 pm (av.). The nine-coordinate Eu center in the tetrameric compound $[Eu(C_6Me_6)(AlCl_4)_2]_4$ exhibits an average Eu−C interaction of 300 pm. The shortening by 6−7 pm compared to **4a** may be explained in terms of a stronger polar attraction between the Eu ion and the arene ring caused by the more electronegative $AlCl_4^-$ ligands.

The molecular structure of the yellow complex $Yb(SAr^*)_2(dme)_2$ (**5**) is shown in Figure 4. The Yb atom has a distorted octahedral coordination, in which the thiolate groups and each DME ligand occupy a *cis* position. The

Table 1. (a) Selected interatomic distances [pm], (b) angles [°], (c) distances from least-square planes [pm], and (d) interplanar angles [°] in $YbI_2(SAr^*)(THF)_3$ (**3**)

| | | | | | | | | |
|---|---|---|---|---|---|---|---|---|
| (a) | | | | | | | | |
| Yb−S | | 258.1(2) | | Yb−O(51) | | 227.0(6) | | |
| Yb−I(1) | | 291.00(9) | | Yb−O(61) | | 227.5(6) | | |
| Yb−I(2) | | 298.40(10) | | S−C(1) | | 177.8(9) | | |
| Yb−O(41) | | 239.0(6) | | | | | | |
| (b) | | | | | | | | |
| I(1)−Yb−I(2) | | 176.74(3) | | I(2)−Yb−O(51) | | 86.2(2) | | |
| S−Yb−O(41) | | 175.9(2) | | I(2)−Yb−O(61) | | 87.5(2) | | |
| S−Yb−O(51) | | 93.7(2) | | O(41)−Yb−O(51) | | 83.9(2) | | |
| S−Yb−O(61) | | 100.0(2) | | O(41)−Yb−O(61) | | 81.9(2) | | |
| S−Yb−I(1) | | 96.81(6) | | O(51)−Yb−O(61) | | 164.5(2) | | |
| S−Yb−I(2) | | 86.45(6) | | Yb−S−C(1) | | 125.1(3) | | |
| I(1)−Yb−O(41) | | 86.8(2) | | S−C(1)−C(6) | | 120.9(7) | | |
| I(1)−Yb−O(51) | | 93.6(2) | | S−C(1)−C(2) | | 120.2(7) | | |
| I(1)−Yb−O(61) | | 91.9(2) | | C(1)−C(2)−C(7) | | 124.8(8) | | |
| I(2)−Yb−O(41) | | 90.0(2) | | C(1)−C(6)−C(22) | | 124.5(8) | | |
| (c)[a] | | | | | | | | |
| C(1)* | C(2)* | C(3)* | C(4)* | C(5)* | C(6)* | S | C(7) | C(22) |
| +2.1 | −0.6 | −1.0 | +1.1 | +0.4 | −2.0 | −14.6 | −14.1 | −12.4 |
| S* | O(41)* | O(51)* | O(61)* | Yb | I(1) | I(2) | | |
| +2.4 | +3.3 | −2.9 | −2.8 | +10.6 | +300.4 | −287.7 | | |
| (d)[b] | | | | | | | | |
| A/B | 74.5 | A/C | 73.0 | A/D | 88.8 | | | |

[a] Atoms marked with an asterisk define the least-square plane. − [b] Least-square planes defined by the following atoms: A: C(1) to C(6); B: C(7) to C(12); C: C(22) to C(27); D: C(1), S, Yb.

rather different S(1)−Yb−S(2), O(82)−Yb−O(85), and O(92)−Yb−O(95) angles of 141.3(1)°, 64.8(2)°, and 65.1(2)°, respectively, reveal a severe distortion from the ideal octahedral environment. The Yb−S bond length of 273.9 pm and the average Yb−O distances of 248.0 pm may be compared with the corresponding values of 275.6(8) pm and 253.5 pm in the related complex $Yb(SMes^*)_2(dme)_2$.[32] Apparently, the slightly shorter distances in **5** are compensated by the more acute S−Yb−S angle of 124.4(2)° in the latter.

Although the Ar* and Mes* substituents are of similar size, they often induce different oligomerization and solvent complexation behavior, as has been noted previously.[16] In contrast to the structures of **4a** and **4b**, the interplanar angles between the M−S−C planes and the central $C_6H_3$ arene rings, i.e. A/D and E/H (Table 3), are close to 90°, which is a consequence of repulsive forces between the DME ligands and the *ortho*-Trip groups.

It is interesting to compare the molecular structures of **3**, **4a**, **4b**, and **5** in terms of the different degrees of steric crowding. Thus, the average M−S−C angle increases from 115° and 116° in **4b** and **4a**, through 125° in **3**, up to 146° in **5**. Furthermore, the average displacement of the *ipso*-Trip carbon atoms [i.e. C(7), C(22), C(43), and C(58)] from the central $C_6H_3$ plane increases in the order **4a** (8.2 pm), **4b** (9.6 pm), **3** (13.3 pm), and **5** (22.9 pm). Apparently, the maximum steric congestion is observed for compound **5**.

### Spectroscopic Characterization

The diamagnetic complexes **4b** and **5** have been characterized by $^1H$ and $^{13}C$ NMR spectroscopy. In addition, compounds **2b**, **4b**, and **5** have been examined by $^{171}Yb$ NMR spectroscopy (Table 6). The $^{171}Yb$ NMR spectrum of an in situ prepared solution of **2b** in $[D_8]THF$ shows a main signal at $\delta = 351$. Smaller resonances of equal height at $\delta = 281$ and $\delta = 457$ can be assigned to the dithiolato species $Yb(SAr^*)_2(THF)_x$ (**6**) and solvated ytterbium(II) iodide $YbI_2(THF)_4$ (**4b**).[33] In the $^{171}Yb$ NMR spectrum of **4b** in $[D_8]$toluene or $[D_6]$benzene, a sharp resonance is observed at $\delta = 768$. A different chemical shift is found if the aromatic solvent is replaced by an alkane. Thus, a $^{171}Yb$ NMR signal at $\delta = 837$ is observed in $[D_{14}]$methylcyclohexane at 233 K, whereas no $^{171}Yb$ resonance is detectable at ambient temperature. The reaction of purple **4b** with more strongly coordinating solvents such as THF or DME results in a color change to yellow. In the $^{171}Yb$ NMR spectrum, a shift to higher field is observed with resonances at $\delta = 204$ (at 233 K) and $\delta = 281$ for the solvated complexes $Yb(SAr^*)_2(dme)_2$ **5** and $Yb(SAr^*)_2(THF)_x$ **6**, respectively. These values may be compared with the $^{171}Yb$ NMR chemical shifts of the ytterbium(II) thiolate $Yb(SMes^*)_2(dme)_2$ and related selenolates and tellurolates, which are found at lower field, specifically at $\delta = 485$[32] and $\delta = 430-526$,[34] respectively. It is notable that no $^{171}Yb$ NMR signal can be detected for **5** at ambient temperature. Apparently, dynamic processes such as solvent exchange, intermolecular arene coordination, or equilibria due to hindered rotation complicate the interpretation of solution NMR-spectroscopic data for compounds **4b** and **5**. In order to gain more insight into these different processes, variable-temperature $^1H$ NMR experiments were performed. At room temperature, the $^1H$ NMR spectrum of **4b** in $[D_8]$toluene shows only one type of thiolate ligand environment with equivalent Trip

Table 2. (a) Selected interatomic distances [pm], (b) angles [°], (c) distances from least-square planes [pm], (d) and interplanar angles [°] in Eu(SAr*)$_2$ (**4a**) and Yb(SAr*)$_2$ (**4b**)

| | **4a**·(THF)$_{0.5}$ | | **4b**·(C$_6$H$_6$)$_{0.5}$ | |
|---|---|---|---|---|
| (a) | | | | |
| M−S(1) | 281.6(1) | | 268.5(2) | |
| M−S(2) | 281.8(1) | {281.7}[a] | 269.6(2) | {269.1} |
| M···C(7) | 303.7(3) | | 292.2(8) | |
| M···C(8) | 309.4(3) | | 297.1(8) | |
| M···C(9) | 312.8(3) | | 302.8(8) | |
| M···C(10) | 315.0(3) | | 305.2(8) | |
| M···C(11) | 302.4(3) | | 293.3(9) | |
| M···C(12) | 298.8(3) | {307.0} | 287.0(8) | {296.3} |
| M···C(43) | 301.1(3) | | 287.7(8) | |
| M···C(44) | 306.9(3) | | 311.8(8) | |
| M···C(45) | 311.1(3) | | 313.9(8) | |
| M···C(46) | 316.1(3) | | 301.7(8) | |
| M···C(47) | 303.3(3) | | 292.3(8) | |
| M···C(48) | 296.7(3) | {305.9} | 282.4(8) | {298.3} |
| M···X(1)[b] | 273.4 | | 262.3 | |
| M···X(2) | 272.2 | {272.8} | 265.0 | {263.7} |
| (b) | | | | |
| S(1)−M−S(2) | 141.89(4) | | 142.73(8) | |
| Yb−S(1)−C(1) | 115.85(11) | | 115.7(3) | |
| Yb−S(2)−C(37) | 115.40(11) | | 115.0(3) | |
| X(1)−M−X(2) | 166.9 | | 164.5 | |
| S(1)−C(1)−C(2) | 122.3(2) | | 121.7(6) | |
| S(1)−C(1)−C(6) | 119.5(2) | | 119.7(6) | |
| S(2)−C(37)−C(38) | 122.3(3) | | 120.4(6) | |
| S(2)−C(37)−C(42) | 120.4(2) | | 121.2(6) | |
| C(1)−C(2)−C(7) | 120.3(3) | | 119.4(7) | |
| C(1)−C(6)−C(22) | 119.6(3) | | 120.4(7) | |
| C(37)−C(38)−C(43) | 119.9(3) | | 120.9(7) | |
| C(37)−C(42)−C(58) | 119.6(3) | | 121.1(7) | |

(c)[c]

| | C(1)* | C(2)* | C(3)* | C(4)* | C(5)* | C(6)* | S(1) | C(7) | C(22) |
|---|---|---|---|---|---|---|---|---|---|
| **4a**: | +3.0 | −0.9 | −1.7 | +2.2 | +0.0 | −2.6 | +15.0 | −2.8 | −16.2 |
| **4b**: | +3.2 | −1.5 | −1.7 | +3.1 | −1.3 | −1.9 | +17.5 | −10.8 | −20.1 |
| | C(37)* | C(38)* | C(39)* | C(40)* | C(41)* | C(42)* | S(2) | C(43) | C(58) |
| **4a**: | +1.4 | −0.7 | −0.6 | +1.1 | −0.4 | −0.9 | +3.0 | −7.6 | −6.2 |
| **4b**: | +1.4 | −1.5 | +0.4 | +0.7 | −0.8 | −0.2 | +1.0 | −1.1 | −6.3 |

(d)[d]

| | A/B | A/C | E/F | E/G | B/I | F/I | B/F | A/D | E/H |
|---|---|---|---|---|---|---|---|---|---|
| **4a**: | 83.6 | 89.5 | 85.2 | 85.0 | 11.5 | 6.3 | 16.0 | 4.7 | 1.7 |
| **4b**: | 82.0 | 89.0 | 84.2 | 82.7 | 13.6 | 7.3 | 19.5 | 6.7 | 0.3 |

[a] Average values are given in brackets. − [b] X(1) and X(2) define the centroids of the C(7) to C(12) and C(43) to C(48) arene rings, respectively. − [c] Atoms marked with an asterisk define the least-square plane. − [d] Least-square planes defined by the following atoms: A: C(1) to C(6); B: C(7) to C(12); C: C(22) to C(27); D: C(1), S(1), M; E: C(37) to C(42); F: C(43) to C(48); G: C(58) to C(63); H: C(37), S(2), M; I: S(1), M, S(2).

substituents, although the signals are very broad. If the temperature is gradually increased, the linewidth decreases and sharp signals are observed at 358 K. At lower temperatures, two coalescence points were detected at 284 K and 227 K, corresponding to energy barriers of 57.1 kJ mol$^{-1}$ and 46.5 kJ mol$^{-1}$, respectively. A full interpretation of the low-temperature $^1$H NMR spectra has not yet been possible due to their complex nature and overlapping signals. It is clear, however, that below 284 K two different Trip substituent environments exist, as is evident from the appearance of two different resonances for the *m*-Trip protons. This observation can be interpreted in terms of hindered rotation about the S(1)−C(1) or S(2)−C(37) bonds and hence the persistence of the metal−π-arene interactions in solution. In order to exclude additional interactions with the aromatic solvent toluene, further low-temperature $^1$H NMR experiments were performed in [D$_{14}$]methylcyclohexane. In this solvent, a single energy barrier of 54.3 kJ mol$^{-1}$ is found and two signals due to the aromatic protons of the Trip substituents are observed below 263 K. In contrast, the $^1$H NMR spectrum of **5** shows only one set of signals due to the Trip substituents and the coordinated DME molecules in the temperature range 223−300 K.

The weak tendency of **4b** to coordinate THF was examined by additional $^{171}$Yb NMR experiments. As mentioned above, a yellow solution of **4b** in neat [D$_8$]THF shows a

Table 3. (a) Selected interatomic distances [pm], (b) angles [°], (c) distances from least-square planes [pm], and (d) interplanar angles [°] in $Yb(SAr^*)_2(dme)_2$ (**5**)

| | | | |
|---|---|---|---|
| (a) | | | |
| Yb−S(1) | 2.739(2) | Yb−O(85) | 2.477(5) |
| Yb−S(2) | 2.739(3) | Yb−O(92) | 2.510(6) |
| Yb−O(82) | 2.478(6) | Yb−O(95) | 2.461(5) |
| (b) | | | |
| S(1)−Yb−S(2) | 141.25(11) | O(85)−Yb−O(92) | 91.9(2) |
| S(1)−Yb−O(82) | 77.18(16) | O(92)−Yb−O(95) | 65.1(2) |
| S(1)−Yb−O(85) | 100.22(13) | Yb−S(1)−C(1) | 149.0(4) |
| S(1)−Yb−O(92) | 136.93(17) | Yb−S(2)−C(37) | 142.8(3) |
| S(1)−Yb−O(95) | 88.61(13) | S(1)−C(1)−C(6) | 121.0(6) |
| S(2)−Yb−O(82) | 138.08(14) | S(1)−C(1)−C(2) | 120.9(6) |
| S(2)−Yb−O(85) | 87.19(14) | S(2)−C(37)−C(42) | 120.4(6) |
| S(2)−Yb−O(92) | 79.95(14) | S(2)−C(37)−C(38) | 120.9(6) |
| S(2)−Yb−O(95) | 102.00(14) | C(1)−C(2)−C(7) | 122.6(7) |
| O(82)−Yb−O(85) | 64.8(2) | C(1)−C(6)−C(22) | 121.5(7) |
| O(82)−Yb−O(92) | 71.1(2) | C(37)−C(38)−C(43) | 124.1(7) |
| O(82)−Yb−O(95) | 92.7(2) | C(37)−C(42)−C(58) | 122.6(7) |
| O(85)−Yb−O(95) | 152.8(2) | | |

| (c)[a] | | | | | | | | |
|---|---|---|---|---|---|---|---|---|
| C(1)* | C(2)* | C(3)* | C(4)* | C(5)* | C(6)* | S(1) | C(7) | C(22) |
| −3.1 | +2.0 | +0.7 | −2.4 | +1.2 | +1.6 | −1.7 | +22.1 | +21.1 |
| C(37)* | C(38)* | C(39)* | C(40)* | C(41)* | C(42)* | S(2) | C(43) | C(58) |
| +5.1 | −3.5 | −1.5 | +4.7 | −3.2 | −1.8 | +11.1 | −27.6 | −20.9 |

| (d)[b] | | | | | |
|---|---|---|---|---|---|
| A/B | A/C | E/F | E/G | A/D | E/H |
| 89.6 | 89.1 | 71.7 | 78.6 | 82.1 | 87.3 |

[a] Atoms marked with an asterisk define the least-square plane. – [b] Least-square planes defined by the following atoms: A: C(1) to C(6); B: C(7) to C(12); C: C(22) to C(27); D: C(1), S(1), Yb; E: C(37) to C(42); F: C(43) to C(48); G: C(58) to C(63); H: C(37), S(2), Yb.

Table 4. Salient structural parameters for selected europium and ytterbium thiolates

| Compound | Oxid. | c. n.[a] | av. Yb−S [pm] | av. Yb−S−C [°][b] | Ref. |
|---|---|---|---|---|---|
| $Eu_2(STrip)_4(THF)_6$ | +II | 6 | 289.8[c]/301.6[d] | 125[c] | [55] |
| $Eu(SC_5H_4N\text{-}2)_2(py)_4$ | +II | 8 | 304.6 | | [56] |
| $Eu(SC_5H_4N\text{-}2)_2(THF)_2(bipy)$ | +II | 8 | 300.6 | | [56] |
| **4a** | +II | 2 (+ 6) | 281.7 | 116 | |
| $Yb(SMes^*)_2(dme)_2$ | +II | 6 | 275.6 | 125 | [32] |
| $Yb(SPh)_2(py)_4$ | +II | 6 | 282.7 | 102 | [57] |
| $[Yb(\mu\text{-}SPh)(\eta^5\text{-}C_4Me_4P)(THF)_2]_2$ | +II | 7 | 282.6 | | [58] |
| $Yb(SC_5H_4N\text{-}2)_2(py)_3$ | +II | 7 | 288.4 | | [59] |
| **5** | +II | 6 | 273.9 | 146 | |
| **4b** | +II | 2 (+ 6) | 269.1 | 115 | |
| $Yb(SPh)_3(py)_3$ | +III | 6 | 264.7 | | [56] |
| $Yb(STrip)_3(py)_3$ | +III | 6 | 264.8 | 117 | [55] |
| $Yb_2(StBu)_6(bipy)_2$ | +III | 6 | 262.3[c]/274.7[d] | 124 | [60] |
| $Yb(SC_5H_4N\text{-}2)_3(py)_2$ | +III | 8 | 276.1 | | [59] |
| **3** | +III | 6 | 258.1 | 125 | |

[a] Coordination number. – [b] Selected values for monomeric compounds with monodentate ligands. – [c] Terminal ligand. – [d] Bridging ligand.

$^{171}$Yb NMR resonance of δ = 281. In contrast, there is no detectable signal in the $^{171}$Yb NMR spectrum at ambient temperature if a 4:1 mixture of toluene and THF is used as solvent. However, if this purple solution is cooled to 253 K, a color change to yellow is observed and a broad resonance appears at δ = 316 ($w_{1/2}$ = 700 Hz). At 233 K, the signal is shifted to δ = 336 and the linewidth is reduced to 180 Hz. Apparently, if the concentration of THF is too low, the solvated complex $Yb(SAr^*)_2(THF)_x$ (**6**) is only stable at low temperatures. The temperature dependence of the chemical shift for **6** (−0.85 ppm $K^{-1}$) may be compared with other reported values, which typically vary between +2 and −0.5 ppm $K^{-1}$.[34]

In the mass spectra of **4a** and **4b**, intense signals due to the molecular ions were found (base peak for **4b**; rel. intensity of 48% for **4a**). In addition, solutions of **4b** in *n*-pentane (purple) and THF (yellow) were studied by UV/Vis spectro-

Table 5. Salient structural parameters for compounds with europium and ytterbium η6-π-arene coordination

| Compound | Oxid. | Yb−C [pm][a] | Yb−X [pm][b] | Ref. |
|---|---|---|---|---|
| $[Eu(C_6Me_6)(AlCl_4)_2]_4$ | +II | 292(2)−307(2) {300} | {267} | [61] |
| **4a** | +II | 298.8(3)−315.0(3) {307} | 273 | |
| | | 296.7(3)−316.1(3) {306} | 272 | |
| $Yb(C_6Me_6)(AlCl_4)_3$ | +III | 274(4)−301(5) {286} | 248 | [62] |
| $Yb(ODpp)_3$ [c] | +III | 281.4(4)−314.8(6) {296} | 263 | [63] |
| $Yb_2(ODpp)_4$ [d] | +II | 275(3)−318(4) {296} | | [14] |
| $[Yb_2(ODpp)_3]^+$ | +II | 294(1)−315(1) {304} | 270 | [14] |
| | | 287(1)−306(1) {297} | 263 | |
| **4b** | +II | 287.0(8)−305.2(8) {296} | 262 | |
| | | 282.4(8)−313.9(8) {298} | 265 | |

[a] {Av. values}. − [b] X defines the centroid of the arene rings. − [c] Dpp = 2,6-$Ph_2C_6H_3$. − [d] Av. values for two independent molecules.

Table 6. $^{171}$Yb NMR parameters for compounds **1b**, **2b**, **4b**, and **5**

| Compound | Solvent | $T$ [K] | δ [ppm] | $w_{1/2}$ [Hz] |
|---|---|---|---|---|
| **1b** | [$D_8$]THF | 298 | [a] | |
| **2b** | [$D_8$]THF | 298 | 351[b] | 28 |
| **4b** | [$D_6$]benzene | 298 | 768 | 8 |
| **4b** | [$D_{14}$]methylcyclohexane | 298 | [c] | |
| | [$D_{14}$]methylcyclohexane | 233 | 837 | 70 |
| **4b** | [$D_6$]toluene (80%) + [$D_8$]THF (20%) | 298 | [c] | |
| | [$D_6$]toluene (80%) + [$D_8$]THF (20%) | 253 | 316 | 700 |
| | [$D_6$]toluene (80%) + [$D_8$]THF (20%) | 233 | 336 | 180 |
| **4b** | [$D_8$]THF | 298 | 281 | 50 |
| **5** | [$D_{10}$]DME | 298 | [c] | |
| | [$D_{10}$]DME | 233 | 204 | 75 |

[a] No $^{171}$Yb NMR signal besides the resonance for $YbI_2(THF)_4$ (δ = 457) detectable. − [b] Additional smaller signals for the homoleptic species $YbI_2(THF)_4$ (δ = 457, $w_{1/2}$ = 40 Hz) and $Yb(SAr^*)_2(THF)_x$ (δ = 281, $w_{1/2}$ = 70 Hz) were observed. − [c] No $^{171}$Yb NMR signal detectable.

photometry. Absorption maxima were observed at 475/546 nm and 369/417 nm, respectively.

It is know from studies on dimeric lanthanide and actinide aryl oxide complexes $M_2(OAr)_6$ (Ar = 2,6-$i$Pr$_2$C$_6$H$_3$; M = La, Nd, Sm, Er, U) that infrared spectroscopy is a valuable tool for the identification of η6-arene-bridged dimeric structures.[35−37] IR spectroscopy shows distinct differences in the aromatic C=C vibrational modes for the π-bound and *O*-bridged phenoxide ligands in these compounds. Table 7 shows the IR vibrational frequencies for the aromatic stretching modes in compounds **3**, **4a**, **4b**, **5** and the thiol Ar*SH, recorded as Nujol mulls. Two bands in the regions 1604−1606 cm$^{-1}$ and 1565−1569 cm$^{-1}$ are common to all the spectra. Additional stretching modes at 1591/1545 cm$^{-1}$ (**4a**) and 1592/1544 cm$^{-1}$ (**4b**) are observed only in the IR spectra of the donor-free compounds. The latter clearly indicate a weakening of the aromatic C=C bonds, consistent with the presence of π-arene interactions, as observed by X-ray crystallography.

Table 7. Infrared vibrational wavenumbers [cm$^{-1}$] for the ν(C=C) stretching modes in compounds **3**, **4a**, **4b**, and **5** and the thiol Ar*SH

| Compound | ν(C=C) | | | |
|---|---|---|---|---|
| **3** | 1605 | | 1565 | |
| **4a** | 1606 | 1591 | 1569 | 1545 |
| **4b** | 1606 | 1592 | 1568 | 1544 |
| **5** | 1604 | | 1566 | |
| Ar*SH | 1605 | | 1567 | |

## Ab initio Calculations

Previous theoretical studies of lanthanide bonding to arenes have been mainly limited to complexes of the zero-valent metals.[38,39] To gain more insight into the $Eu^{2+}$− or $Yb^{2+}$−arene interactions present in **4a** and **4b**, ab initio calculations on suitable model systems were performed. Quasi-relativistic pseudo-potentials of the Stuttgart/Bonn group were employed for atoms heavier than sulfur.

### (a) [Ln(donor)]$^{2+}$ Species

In order to test the influence of different substituents and to gain a qualitative impression of the magnitude of the $Ln^{2+}$−η6-arene interaction, the simple complexes $[Ln(arene)]^{2+}$ (Ln = Eu, Yb; arene = $C_6H_6$, $C_6F_6$, 1,3,5-$Me_3C_6H_3$, 1,3,5-$i$Pr$_3$C$_6$H$_3$) were first examined. For comparison, the coordination of $Eu^{2+}$ and $Yb^{2+}$ to the strong σ-donors tetrahydrofuran, dimethoxyethane, and the Arduengo-type carbene imidazol-2-ylidene was also investigated. Table 8 summarizes the results of these calculations,

Table 8. B3LYP/6−31G*-optimized bond lengths [pm] and binding energies [kJ mol$^{-1}$] for [Ln(arene)]$^{2+}$, [Ln(THF)]$^{2+}$, [Ln(dme)]$^{2+}$, and [Ln(imidazol-2-ylidene)]$^{2+}$ species (Ln = Eu, Yb)

| Compound | Symm. | Yb−C/O | C−C[a] | $\Delta E_e$ | $\Delta E_{ZPE}$ | $\Delta H_0$ |
|---|---|---|---|---|---|---|
| [Eu($C_6H_6$)]$^{2+}$ | $C_{6v}$ | 298.9 | 141.0 | −277.1 | 3.8 | −273.3 |
| [Eu($C_6F_6$)]$^{2+}$ | $C_{6v}$ | 308.5 | 141.2 | −115.6 | 2.1 | −113.5 |
| [Eu(1,3,5-$Me_3C_6H_3$)]$^{2+}$ | $C_3$ | {293.1}[b] | {141.6} | −334.4 | 3.8 | −330.6 |
| [Eu(1,3,5-$i$Pr$_3C_6H_3$)]$^{2+}$ | $C_3$ | {290.9} | {141.3} | −382.3 | −1.0 | −383.3 |
| [Eu(THF)]$^{2+}$ | $C_2$ | 231.2 | | −297.0 | 2.3 | −294.7 |
| [Eu(dme)]$^{2+}$ | $C_2$ | 241.0 | | −428.3 | 5.1 | −423.2 |
| [Eu(imidazol-2-ylidene)]$^{2+}$ | $C_{2v}$ | 258.8 | | −386.2 | 6.5 | −379.7 |
| [Yb($C_6H_6$)]$^{2+}$ | $C_{6v}$ | 287.9 | 141.1 | −305.3 | 3.6 | −301.7 |
| [Yb($C_6F_6$)]$^{2+}$ | $C_{6v}$ | 297.1 | 141.4 | −134.2 | 1.9 | −132.3 |
| [Yb(1,3,5-$Me_3C_6H_3$)]$^{2+}$ | $C_3$ | {282.6} | 141.7 | −366.4 | 3.6 | −362.8 |
| [Yb(1,3,5-$i$Pr$_3C_6H_3$)]$^{2+}$ | $C_3$ | {280.7} | 141.3 | −420.7 | −1.4 | −422.1 |
| [Yb(THF)]$^{2+}$ | $C_2$ | 222.5 | | −325.8 | 2.4 | −323.4 |
| [Yb(dme)]$^{2+}$ | $C_2$ | 231.6.0 | | −470.2 | 5.4 | −464.8 |
| [Yb(imidazol-2-ylidene)]$^{2+}$ | $C_{2v}$ | 249.1 | | −425.7 | 6.5 | −419.2 |

[a] For the isolated arenes, the following C−C distances were obtained at the B3LYP/6−31G* level of theory: 139.7 ($C_6H_6$), 139.4 ($C_6F_6$), {139.9} (1,3,5-$Me_3C_6H_3$) {140.0} (1,3,5-$i$Pr$_3C_6H_3$). − [b] {Av. values}.

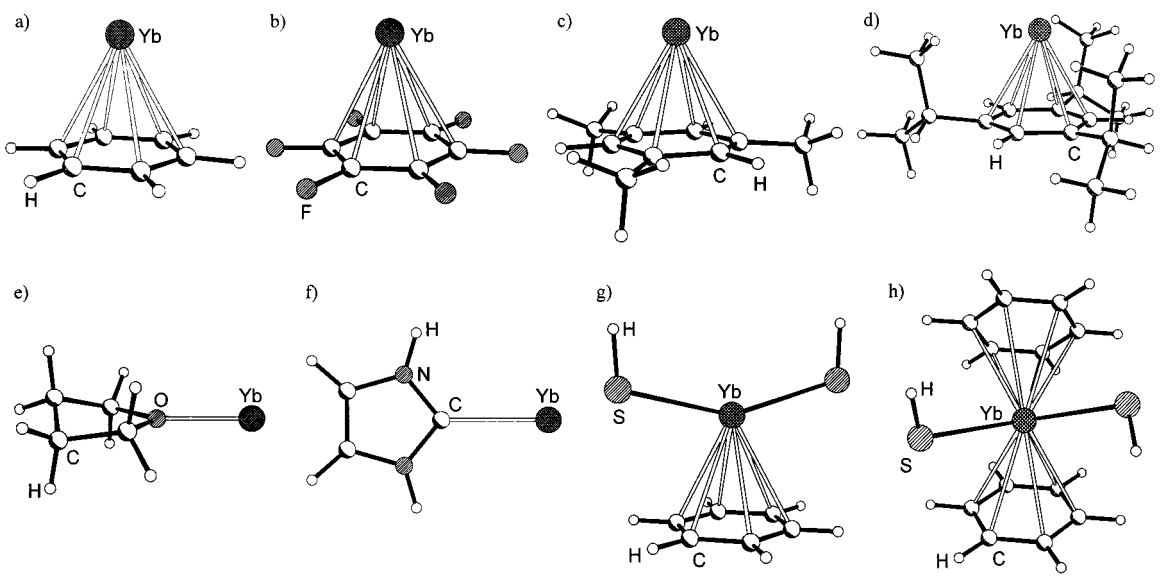


Figure 5. Optimized structures for the model compounds (a) [Yb($C_6H_6$)]$^{2+}$, (b) [Yb($C_6F_6$)]$^{2+}$, (c) [Yb(1,3,5-$Me_3C_6H_3$)]$^{2+}$, (d) [Yb(1,3,5-$i$Pr$_3C_6H_3$)]$^{2+}$, (e) [Yb(THF)]$^{2+}$, (f) [Yb(imidazol-2-ylidene)]$^{2+}$, (g) [Yb(SH)$_2$($C_6H_6$)], and (h) [Yb(SH)$_2$($C_6H_6$)$_2$]; calculations were either performed at the B3LYP/6−31G* [(a)−(f)] or the MP2/6−31G* [(g), (h)] level of theory

which were performed at the B3LYP/6−31G* level of theory. The optimized structures of the Yb$^{2+}$ adducts are shown in Figure 5 (a)−(f). Obviously, the binding energy largely depends on the electron-withdrawing or -donating ability of the substituents on the arene rings, as would be expected for a cation−arene interaction dominated by electrostatics. Therefore, as a result of the strong $-I$ effect of the fluorine atoms, the smallest binding energy ($\Delta H_0$) of −113.5 kJ mol$^{-1}$ is calculated for the compound [Eu($C_6F_6$)]$^{2+}$, whereas a value of −273.3 kJ mol$^{-1}$ is calculated for the benzene complex [Eu($C_6H_6$)]$^{2+}$. The introduction of electron-donating alkyl groups leads to a substantial increase in $\Delta H_0$ from −330.6 kJ mol$^{-1}$ for [Eu(1,3,5-$Me_3C_6H_3$)]$^{2+}$ to −383.3 kJ mol$^{-1}$ for [Eu(1,3,5-$i$Pr$_3C_6H_3$)]$^{2+}$. With a value of 297 kJ mol$^{-1}$, the dissociation energy of the adduct [Eu(THF)]$^{2+}$ is intermediate between the values for [Eu($C_6H_6$)]$^{2+}$ and [Eu(1,3,5-$Me_3C_6H_3$)]$^{2+}$. This is in accordance with the experimental observation that intramolecular arene binding in **4a** and **4b** is favored over the coordination of THF. It is notable that the binding energy for the interaction of Eu$^{2+}$ with the Arduengo-type carbene imidazol-2-ylidene is substantially larger than that for the coordination of THF and comparable to that for coordination of the arene 1,3,5-$i$Pr$_3C_6H_3$. Therefore, it should be possible to obtain adducts of **4a** or **4b** with substituted carbenes of the imidazol-2-ylidene type. As one might expect, the greatest dissociation energy of 423 kJ mol$^{-1}$ is found for the compound [Eu(dme)]$^{2+}$. This is in agreement with the isolation of the bis(DME) adduct **5**. Compared to the corresponding Eu$^{2+}$ compounds, the binding energies of the Yb$^{2+}$ complexes are increased by 9−14%, which is attributable to the smaller ionic radius of

Table 9. Calculated bond lengths [pm], bond angles [°], torsion angles [°], and energies [Hartree] for $Yb(SH)_2$ species (see below) at different levels of theory

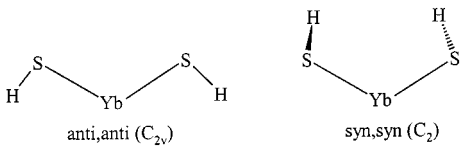


| Compound | Symm. | Yb−S | S−Yb−S | S−H | H−S−Yb | H−S−Yb−S | $E_e$ | $E_{ZPE}$ |
|---|---|---|---|---|---|---|---|---|
| | B3LYP/6−31G* | | | | | | | |
| $Yb(SH)_2$ *anti*/*anti* | $C_{2v}$ | 270.5 | 132.1 | 135.7 | 96.7 | 180 | −830.601965 | 0.015359 |
| $Yb(SH)_2$ *syn*/*syn* | $C_2$ | 269.0 | 128.5 | 135.4 | 98.4 | 3.4 | −830.604450 | 0.015495 |
| | B3LYP/6−31+G** | | | | | | | |
| $Yb(SH)_2$ *anti*/*anti* | $C_{2v}$ | 270.8 | 133.9 | 135.3 | 95.9 | 180 | −830.612178 | 0.015359 |
| $Yb(SH)_2$ *syn*/*syn* | $C_2$ | 269.2 | 128.8 | 135.0 | 97.8 | 3.5 | −830.614476 | 0.015489 |
| | MP2/6−31G* | | | | | | | |
| $Yb(SH)_2$ *anti*/*anti* | no minimum | | | | | | | |
| $Yb(SH)_2$ *syn*/*syn* | $C_2$ | 270.6 | 149.7 | 134.5 | 101.7 | 20.2 | −829.238995 | 0.015563 |
| | MP2/6−31+G** | | | | | | | |
| $Yb(SH)_2$ *syn*/*syn* | $C_2$ | 271.3 | 152.1 | 133.6 | 97.2 | 34.3 | −829.267290 | 0.015833 |

the latter. In accordance with the electronic properties of the various arene ligands, the metal···C(arene) distances also vary considerably by 16−17 pm, being shortest in $[M(1,3,5\text{-}iPr_3C_6H_3)]^{2+}$ and longest in $[M(C_6F_6)]^{2+}$. A notable feature of the calculated $[M(1,3,5\text{-}iPr_3C_6H_3)]^{2+}$ structures is the presence of three agostic-type M···H interactions to C−H bonds of the isopropyl groups (Eu···H: 296.2 pm; Yb···H: 285.5 pm). The shortest experimentally determined M···H distances in **4a** and **4b** are 303 pm and 301 pm, respectively.

### (b) $Yb(SH)_2$

DFT calculations with two different basis sets revealed at least two stable conformers (Table 9). The U-shaped *syn*,*syn* species with $C_2$ symmetry is energetically favored by ca. 6 kJ mol$^{-1}$ over the W-shaped *anti*,*anti* conformer ($C_{2v}$). According to MP2 results, only the former is a minimum on the potential-energy surface. The bending angle at the Yb center and the Yb−S distance were computed at MP2/6−31+G** level to be 152.1° and 271.3 pm, respectively. The DFT calculations showed slightly shorter Yb−S bonds and a more acute S−Yb−S angle of ca. 130° for both conformers. The occurrence of bent equilibrium geometries for some lanthanide $MX_2$ species[40,41] and related compounds of the heavier alkaline earth elements[42,43] is now well established. This bending can be explained by the presence of small σ-bonding contributions (involving metal d orbitals) and/or the polarization of the metal cation by the ligands. According to Kaupp et al., the $MX_2$ compounds can be divided into molecules with genuinely bent structures [for example, $EuF_2$, $Ba(CH_3)_2$] and molecules with quasi-linear equilibrium geometries (for example, $SmCp_2$, $CaF_2$). The latter show almost no energy change (< 1−2 kJ mol$^{-1}$) when the equilibrium angle is increased to 180°, whereas the former exhibit considerable linearization energies of up to 33 kJ mol$^{-1}$.

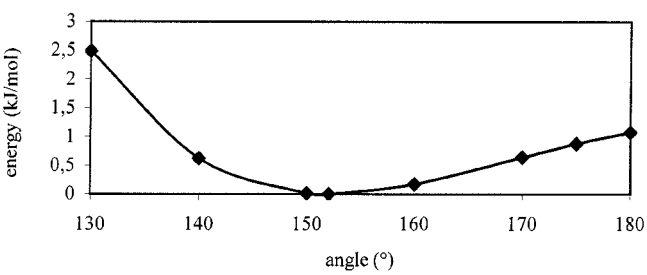


Figure 6. Bending potential curve for *syn*/*syn* $Yb(SH)_2$ at the MP2/6−31+G** level of theory

Figure 6 shows the rather shallow bending potential curve for *syn*/*syn* $Yb(SH)_2$ calculated at the MP2/6-31+G** level of theory. With a linearization energy of 1.1 kJ mol$^{-1}$, it can be classified as a quasi-linear molecule.

### (c) $Yb(SH)_2(C_6H_6)_n$ Complexes ($n$ = 1, 2)

Calculated bond parameters and binding energies for $Yb(SH)_2(C_6H_6)$ and $Yb(SH)_2(C_6H_6)_2$ species, both of which were computed at the B3LYP and MP2 levels of theory using the 6−31G* basis set, are summarized in Table 10. The MP2-optimized structures are shown in Figure 5 (g) and (h). Compared to the experimentally determined distances in complex **4b**, the calculated Yb−S bond lengths for the model compound $Yb(SH)_2(C_6H_6)_2$ are overestimated by 5.1 pm (MP2) and 7.1 pm (B3LYP), respectively. The difference between the DFT-computed and observed Yb···C distances is quite substantial, amounting to +22.3 pm. A much better description is provided by the MP2 calculation, which overestimates the distance of the Yb···arene interaction by only 5.6 pm. Replacing the coordinated benzene in $Yb(SH)_2(C_6H_6)_2$ by the substituted arene $1,3,5\text{-}iPr_3C_6H_3$ can be expected to result in a further reduction in the Yb···C distances, which might, however, be partly compensated by repulsion between the isopropyl groups. The dissociation enthalpy corresponding to the reaction

Table 10. Calculated bond lengths [pm], bond angles [°], torsion angles [°], and binding energies [kJ mol$^{-1}$] for $Yb(SH)_2(C_6H_6)$ and $Yb(SH)_2(C_6H_6)_2$ species at different levels of theory

| Compound[a] | Symm. | Yb−C[b] | Yb−S | S−Yb−S | H−S−Yb−S | $\Delta E_e$ | $\Delta E_{ZPE}$ | $\Delta H_0$ [c] |
|---|---|---|---|---|---|---|---|---|
| | B3LYP/6−31G* | | | | | | | |
| $Yb(SH)_2(C_6H_6)$ | $C_2$ | {310.5} | 272.9 | 139.1 | 0.4 | −70.8 | +4.4 | −66.4 |
| $Yb(SH)_2(C_6H_6)_2$ | $C_2$ | {319.6} | 276.2 | 124.5 | 44.0 | −105.2 | +7.3 | −97.9 |
| | MP2/6−31G* | | | | | | | |
| $Yb(SH)_2(C_6H_6)$ | $C_2$ | {298.1} | 271.8 | 149.9 | 0.02 | −108.3 | +4.6[d] | −103.7 |
| $Yb(SH)_2(C_6H_6)_2$ | $C_2$ | {302.9} | 274.2 | 126.6 | 52.4 | −185.4 | +7.8[d] | −177.6 |

[a] *syn*/*syn* isomers only. − [b] {Av. values}. − [c] According to the reaction $Yb(SH)_2 + n\ C_6H_6 \rightarrow Yb(SH)_2(C_6H_6)_n$. − [d] $E_{ZPE}$ was taken from the DFT calculation above.

$Yb(SH)_2(C_6H_6)_2 \rightarrow Yb(SH)_2(C_6H_6) + C_6H_6$ was estimated to be 31.5 kJ mol$^{-1}$ (B3LYP) and 73.9 kJ mol$^{-1}$ (MP2). These values may be compared with the NMR-spectroscopically determined energy barriers of 57.1 kJ mol$^{-1}$ and 54.3 kJ mol$^{-1}$ found for solutions of **4b** in [$D_8$]toluene or [$D_{14}$]methylcyclohexane.

## Conclusion

The use of the very bulky *m*-terphenyl-substituted Ar*S ligand has permitted the synthesis of the first monomeric σ-donor-free lanthanide(II) thiolates. In the solid state, steric saturation of the europium and ytterbium centers is achieved by two $\eta^6$-π-arene interactions, as has been demonstrated by X-ray structural analysis and IR spectroscopy. Evidence that these interactions also persist in solution has been provided by variable-temperature NMR experiments, which show an energy barrier of 54.3 kJ mol$^{-1}$ for **4b** in methylcyclohexane solution. In contrast, the $^1$H NMR spectrum of the bis(DME) adduct **5** shows no dynamic character in the temperature range 223−300 K, despite the more crowded environment of the Yb center. From ab initio calculations on the model system $Yb(SH)_2(C_6H_6)_2$, it has been estimated that the dissociation of one molecule of benzene requires between 31.5 and 73.9 kJ mol$^{-1}$ depending on the method used.

## Experimental Section

**General:** All manipulations were performed using standard Schlenk techniques under purified argon. Solvents were freshly distilled under argon from Na wire or $LiAlH_4$. The compounds $Yb[N(SiMe_3)_2]_2$ [17] and Ar*SH[44] were synthesized according to known literature procedures. − NMR spectra were recorded with Bruker AM 200, AC250, and AM 400 instruments and were referenced to solvent resonances ($^1$H, $^{13}$C) or $YbCp^*_2(THF)_2$ [34] ($^{171}$Yb). − UV spectra were recorded with a Bruins Omega 10 spectrophotometer. − IR spectra were recorded in the range 4000−200 cm$^{-1}$ with a Perkin−Elmer Paragon 1000 PC spectrometer. − Mass spectra were measured with a Varian MAT711 instrument. − Melting points were determined under Ar in sealed glass tubes.

**$Yb(SAr^*)I_2(THF)_3$ (3):** A solution of **2b** was prepared from Ar*SH (1.76 g, 3.41 mmol), Yb chips (0.59 g, 3.41 mmol), and 2-iodobenzotrifluoride (0.48 mL, 3.41 mmol) as described below for the synthesis of **4b**. With stirring, a solution of iodine (0.42 g, 3.31 mmol) in THF was added dropwise at 0 °C. The mixture was allowed to warm to ambient temperature and ca. 30 mL of *n*-heptane was added. After filtration through a glass filter frit, the resulting purple solution was concentrated until crystallization commenced and then stored in a freezer at ca. −25 °C for 2 d to give **3** as purple crystals (2.25 g, 57%); m.p. 120−240 °C (dec., compound gradually decolorizes). − IR (CsBr, Nujol): $\tilde{\nu}$ = 1605 ms, 1565 m, 1358 s, 1345 sh, 1315 ms, 1299 s, 1247 m, 1166 ms, 1154 mw, 1130 mw, 1115 m, 1098 m, 1068 ms, 1037 s, 1000 vs, 954 w, 940 m, 916 m, 878 s, 851 sh, 835 vs, 800 s, 774 s, 745 s, 732 s, 674 m, 663 mw, 650 ms, 608 w, 590 w, 526 m, 508 w, 427 mw, 410 cm$^{-1}$ w. − $C_{48}H_{73}I_2O_3SYb$ (1157.0): calcd. C 49.83, H 6.36; found C 49.50, H 6.38.

**$Eu(SAr^*)_2$ (4a):** At 0 °C, an Eu ingot (3.9 g, 25.7 mmol) was added to a stirred solution of Ar*SH (1.08 g, 2.10 mmol) and 2-iodobenzotrifluoride (0.48 mL, 3.41 mmol) in THF (60 mL). Stirring was continued for 1 h at 0 °C and for a further 1 h at 20 °C, whereupon the resulting light-orange solution was carefully decanted from the excess Eu metal. The volume of the solution was reduced to ca. 5 mL and *n*-heptane (ca. 20 mL) was added. After separation from the precipitated $EuI_2(THF)_5$, the remaining solution was concentrated in vacuo until crystallization commenced. Storage in a freezer at 5 °C overnight afforded **4a**·$(THF)_{0.5}$ as orange crystals (0.89 g, 70%); m.p. 289−292 °C (compound softens > 216 °C). − IR (CsBr, Nujol): $\tilde{\nu}$ = 1606 m, 1591 m, 1569 ms, 1545 m, 1411 m, 1363 s, 1336 m, 1314 ms, 1249 ms, 1167 ms, 1150 m, 1110 ms, 1081 m, 1069 ms, 1049 vs, 1003 m, 939 ms, 922 m, 886 vs, 870 s, 850 w, 791 s, 775 m, 756 m, 738 vs, 733 vs, 649 ms, 612 w, 587 m, 562 w, 519 ms, 426 w, 360 cm$^{-1}$ m. − EI-MS (70 eV): *m*/*z* (%) = 1179.7 (48) [$Eu(SAr^*)_2^+$], 666.3 (100) [$EuSAr^{*+}$], 514.4 (77) [$SAr^{*+}$]. − $C_{74}H_{102}EuO_{0.5}S_2$ (1215.7): calcd. C 73.11, H 8.46; found C 72.91, H 8.72.

**$Yb(SAr^*)_2$ (4b). − Method A:** Ar*SH (0.26 g, 0.50 mmol) was added through a solid-addition tube to a stirred solution of $Yb[N(SiMe_3)_2]_2$ (0.12 g, 0.24 mmol) in *n*-pentane (ca. 15 mL). The reaction mixture was stirred for a further 30 min and then the solvent was removed under reduced pressure. The intensely colored residue was redissolved in a mixture of *n*-heptane and a small amount of benzene. Cooling in a freezer at 5 °C afforded **4b**·$(C_6H_6)_{0.5}$ as purple crystals (0.19 g, 64%), which were suitable for X-ray crystallographic studies. The solvate-free compound **1** was obtained by pumping at $10^{-3}$ mbar for 2 h. − **Method B:** Ar*SH (2.06 g, 4.00 mmol) and Yb chips (1.1 g, 6.36 mmol) were suspended in THF (60 mL) at 0 °C. With stirring, 2-iodobenzotrifluoride (0.56 mL, 4.00 mmol) was added dropwise and after a short induction period a color change to orange was observed. Stirring was con-

tinued for 2 h, whereupon the resulting maroon solution was carefully decanted from the unchanged excess Yb metal. Most of the solvent was removed under reduced pressure and the concentrate was treated with *n*-pentane (50 mL). The solution was separated from the precipitated greenish-yellow $YbI_2(THF)_4$ and all volatile materials were distilled off in vacuo. Recrystallization of the purple-brown residue from *n*-heptane/toluene (20:1) followed by pumping at $10^{-3}$ mbar for 2 h gave pure **4b** as a purple powder (1.58 g, 66%); m.p. 263−265 °C (compound softens > 220 °C). − $^1$H NMR (250.1 MHz, [D$_8$]toluene, 85 °C): δ = 1.06 [d, $^3J_{HH}$ = 6.9 Hz, 24 H, *o*/*p*-CH(C*H*$_3$)$_2$], 1.24 [d, $^3J_{HH}$ = 6.9 Hz, 24 H, *o*/*p*-CH(C*H*$_3$)$_2$], 1.31 [d, $^3J_{HH}$ = 6.9 Hz, 24 H, *o*/*p*-CH(C*H*$_3$)$_2$], 2.89 [sept, $^3J_{HH}$ = 6.9 Hz, 8 H, *o*-C*H*(CH$_3$)$_2$], 3.07 [sept, $^3J_{HH}$ = 6.9 Hz, 4 H, *p*-C*H*(CH$_3$)$_2$], 6.86 (m, 6 H, *m*/*p*-C$_6$H$_3$), 7.17 (s, 8 H, *m*-Trip). − $^{13}$C NMR (62.9 MHz, [D$_8$]toluene, 85 °C): δ = 23.8, 24.3, 24.8 [*o*/*p*-CH(*C*H$_3$)$_2$], 31.2 [*o*-*C*H(CH$_3$)$_2$], 34.0 [*p*-*C*H(CH$_3$)$_2$], 120.6 (*p*-C$_6$H$_3$), 122.0 (*m*-Trip), 129.0 (*m*-C$_6$H$_3$), 141.6, 142.7 (*i*-Trip, *o*-C$_6$H$_3$), 148.3 (*o*-Trip), 149.3 (*p*-Trip), 152.5 (*i*-C$_6$H$_3$). − $^{171}$Yb NMR (70.1 MHz, [D$_6$]benzene, 25 °C): δ = 768 ($w_{1/2}$ = 8 Hz) − IR (CsBr, Nujol): $\tilde{\nu}$ = 1606 m, 1592 m, 1568 m, 1544 m, 1314 ms, 1249 ms, 1168 ms, 1150 m, 1110 ms, 1082 m, 1069 m, 1049 s, 1004 w, 939 s, 920 m, 886 vs, 869 vs, 849 w, 791 vs, 774 m, 755 ms, 740 vs, 733 vs, 650 s, 611 w, 587 m, 519 s, 425 w, 363 m, 306 cm$^{-1}$ w. − EI-MS (70 eV): *m*/*z* (%) = 1200.7 (100) [Yb(SAr*)$_2^+$], 687.3 (32) [YbSAr*$^+$], 514.4 (19) [SAr*$^+$]. − $C_{72}H_{98}S_2Yb$ (1200.74): calcd. C 72.02, H 8.23; found C 71.41, H 8.36. − UV/Vis (*n*-pentane): $\lambda_{max}$ (ε) = 475 nm (110 M$^{-1}$ cm$^{-1}$), 546 (90). − UV/Vis (THF): $\lambda_{max}$ (ε) = 369 nm (480 M$^{-1}$ cm$^{-1}$), 417 (250).

**Yb(SAr*)$_2$(THF)$_x$ (6):** $^1$H NMR (200.13 MHz, [D$_8$]THF, 25 °C): δ = 0.95 [d, $^3J_{HH}$ = 6.8 Hz, 24 H, *o*/*p*-CH(C*H*$_3$)$_2$], 1.16 [d, $^3J_{HH}$ = 6.8 Hz, 24 H, *o*/*p*-CH(C*H*$_3$)$_2$], 1.26 [d, $^3J_{HH}$ = 6.8 Hz, 24 H, *o*/*p*-CH(C*H*$_3$)$_2$], 2.86 [sept, $^3J_{HH}$ = 6.8 Hz, 4 H, *p*-C*H*(CH$_3$)$_2$], 2.95 [sept, $^3J_{HH}$ = 6.8 Hz, 8 H, *o*-C*H*(CH$_3$)$_2$], 6.67 (m, 6 H, *m*/*p*-C$_6$H$_3$), 6.93 (s, 8 H, *m*-Trip). − $^{13}$C NMR (50.33 MHz, [D$_8$]THF, 25 °C): δ = 24.5, 24.5, 25.8 [*o*/*p*-CH(*C*H$_3$)$_2$], 31.2 [*o*-*C*H(CH$_3$)$_2$], 34.9 [*p*-*C*H(CH$_3$)$_2$], 119.3 (*p*-C$_6$H$_3$), 121.1 (*m*-Trip), 129.9 (*m*-C$_6$H$_3$), 142.9, 144.4 (*i*-Trip, *o*-C$_6$H$_3$), 146.3 (*p*-Trip), 147.3 (*o*-Trip), 152.5 (*i*-C$_6$H$_3$). − $^{171}$Yb NMR (70.1 MHz, [D$_8$]THF, 25 °C): δ = 281 ($w_{1/2}$ = 50 Hz). − $^{171}$Yb NMR {70.1 MHz, [D$_8$]toluene (ca. 80%) + [D$_8$]THF (ca. 20%), −40 °C}: δ = 336 ($w_{1/2}$ = 180 Hz).

**Yb(SAr*)$_2$(dme)$_2$ (5):** In a Schlenk tube, purple **4b** (0.35 g, 0.29 mmol) was treated with two drops of DME, which immediately gave **5** as a yellow, microcrystalline material in quantitative yield. The excess DME was carefully removed in vacuo at 0 °C. Prolonged pumping at $10^{-3}$ mbar overnight gave **4b** once more. Crystals of **5** suitable for X-ray crystallographic studies were obtained from an *n*-pentane/DME mixture (5:1) at −25 °C; m.p.: compound darkens > ca. 110 °C and melts to a purple-brown liquid between 265 and 270 °C. After cooling to ambient temperature and standing for 1 h, the upper crust of the solid turns yellow again. − $^1$H NMR (250.1 MHz, [D$_{10}$]DME, 25 °C): δ = 0.97 [d, $^3J_{HH}$ = 6.8 Hz, 24 H, *o*/*p*-CH(C*H*$_3$)$_2$], 1.18 [d, $^3J_{HH}$ = 6.8 Hz, 24 H, *o*/*p*-CH(C*H*$_3$)$_2$], 1.25 [d, $^3J_{HH}$ = 6.8 Hz, 24 H, *o*/*p*-CH(C*H*$_3$)$_2$], 2.87 [m, 12 H, *o*- + *p*-C*H*(CH$_3$)$_2$], 3.27 (s, 12 H, OCH$_3$), 3.43 (s, 8 H, OCH$_2$) [these two signals correspond to the coordinated non-deuterated DME; another set of signals is observed for the perdeuterated solvent], 6.67 (m, 6 H, *m*- + *p*-C$_6$H$_3$), 6.88 (s, 8 H, *m*-Trip). − $^{171}$Yb NMR (70.1 MHz, [D$_{10}$]DME, −40 °C): δ = 204 ($w_{1/2}$ = 75 Hz). − IR (CsBr, Nujol): $\tilde{\nu}$ = 1604 m, 1566 ms, 1358 s, 1315 ms, 1276 w, 1243 ms, 1209 w, 1190 m, 1168

Table 11. Selected crystallographic data for compounds **3**, **4a**, **4b**, and **5**

| Compound[a] | **3** | **4a**·(THF)$_{0.5}$ | **4b**·(C$_6$H$_6$)$_{0.5}$ | **5** |
|---|---|---|---|---|
| Empirical formula | $C_{48}H_{73}I_2O_3SYb$ | $C_{74}H_{102}S_2Eu$ | $C_{75}H_{101}S_2Yb$ | $C_{80}H_{118}O_4S_2Yb$ |
| Molecular mass | 1157.0 | 1215.6 | 1239.7 | 1380.9 |
| Color, habit | purple, plate | deep orange, block | purple, block | yellow, needle fragment |
| Crystal size [mm] | 0.45 × 0.20 × 0.05 | 0.70 × 0.40 × 0.35 | 0.75 × 0.65 × 0.60 | 0.40 × 0.30 × 0.30 |
| Crystal system | orthorhombic | triclinic | triclinic | monoclinic |
| Space group | $P2_12_12_1$ | $P\bar{1}$ | $P\bar{1}$ | $P2_1$ |
| *a* [Å] | 13.543(3) | 13.278(2) | 13.028(5) | 13.905(3) |
| *b* [Å] | 15.984(3) | 14.537(3) | 14.270(6) | 18.837(4) |
| *c* [Å] | 23.448(5) | 18.804(4) | 18.681(8) | 15.329(3) |
| α [°] | 90 | 105.60(2) | 106.63(3) | 90 |
| β [°] | 90 | 95.18(1) | 96.02(2) | 107.56(2) |
| γ [°] | 90 | 97.80(1) | 96.61(2) | 90 |
| *V* [Å$^3$] | 5076(2) | 3433(1) | 3271(2) | 3828(1) |
| *Z* | 4 | 2 | 2 | 2 |
| $d_{calcd.}$ [g cm$^{-3}$] | 1.514 | 1.176 | 1.259 | 1.198 |
| μ [cm$^{-1}$] | 31.35 | 10.13 | 15.34 | 13.21 |
| 2θ range [°] | 3−54 | 4−54 | 4−50 | 3−54 |
| Unique data/$R_{int}$ | 6727/0.0630 | 14752/0.0373 | 11176/0.0652 | 9449/0.0466 |
| Data with $I > 2\sigma(I)$ ($N_o$) | 5499 | 11454 | 8311 | 7449 |
| Parameters ($N_p$) | 527 | 832 | 828 | 829 |
| $R1$ [$I > 2\sigma(I)$][b] | 0.0436 | 0.0419 | 0.0671 | 0.0479 |
| $wR2$ (all data)[c] | 0.0848 | 0.1018 | 0.1818 | 0.1033 |
| GoF[d] | 1.213 | 0.956 | 1.225 | 1.206 |
| Largest diff. peak and hole [e·Å$^{-3}$] | 0.62/−0.83 | 1.10/−0.83 | 1.78/−1.62 | 1.19/−0.60 |

[a] All data were collected at 173 K using Mo-$K_\alpha$ (λ = 0.71073 Å) radiation. − [b] $R1 = (||F_o| - |F_c||)/|F_o|$. − [c] $wR2 = \{[w(F_o^2 - F_c^2)^2]/[w(F_o^2)^2]\}^{1/2}$. − [d] GoF = $\{[w(F_o^2 - F_c^2)^2]/(N_o - N_p)\}$.

m, 1128 w, 1111 ms, 1059 vs, 1051 sh, 1025 ms, 1005 m, 954 w, 941 m, 920 w, 875 s, 872 s, 868 s, 860 s, 831 m, 794 s, 775 m, 755 w, 742 vs, 736 vs, 650 ms, 608 w, 588 w, 567 w, 520 m, 425 mw, 379 $cm^{-1}$ mw. – $C_{80}H_{118}O_4S_2Yb$ (1381.0): calcd. C 69.58, H 8.61; found C 69.42, H 8.71.

**X-ray Crystallography:** X-ray-quality crystals were obtained as described above. Crystals were removed from Schlenk tubes and immediately covered with a layer of viscous hydrocarbon oil (Paratone N, Exxon). A suitable crystal was selected, attached to a glass fibre, and instantly placed in a low-temperature $N_2$ stream.[45] All data were collected at 173 K using either a Syntex $P2_1$ (**3**, **5**) or a Siemens P4 (**4a**, **4b**) diffractometer. Crystal data are given in Table 11. Calculations were carried out with the SHELXTL PC 5.03[46] and SHELXL-97[47] program systems installed on a local PC. The structures were solved by direct methods and refined against $F_o^2$ by full-matrix least-squares techniques. An absorption correction was applied by using semiempirical ψ-scans (**5**) or the program XABS2[48] (**3**, **4b**). For **4a**, no absorption correction was used. Anisotropic thermal parameters were included for all non-hydrogen atoms with the exception of the co-crystallized THF molecule, which was refined with a common isotropic $U$ value. The methyl carbon atoms of two (**5**) or four (**4a**, **4b**) disordered isopropyl groups were refined with split positions. The geometries of the disordered isopropyl groups and the co-crystallized benzene molecule (**4b**) were restrained with SADI and DFIX commands. H atoms were placed in geometrical positions and were refined using a riding model that included free rotation of the methyl groups. Their isotropic thermal parameters were either allowed to refine or were constrained to 1.2 (aryl H) or 1.5 (methyl groups) times $U_{eq}$ of the carbon atom to which they were bound. Final $R$ values are listed in Table 11. Salient bond lengths and angles are given in Tables 1–3. Crystallographic data (excluding structure factors) for the structures reported in this paper have been deposited with the Cambridge Crystallographic Data Centre as supplementary publication nos. CCDC-150909 (**3**), -150907 (**4a**), -150908 (**4b**), and -150910 (**5**). Copies of the data can be obtained free of charge on application to the CCDC, 12 Union Road, Cambridge CB2 1EZ, U.K. [Fax: (internat.) + 44-1223/336-033; E-mail: deposit@ccdc.cam.ac.uk].

**Computational Details:** The Gaussian 98[49] package was used for all energy and frequency calculations. The geometries of the molecules were optimized using either density functional theory (DFT) with the functional B3LYP or second-order Møller–Plesset perturbation theory (MP2). Quasi-relativistic 11- or 10-valence-electron pseudo-potentials of the Stuttgart/Bonn group were employed for the heavy atoms Sc,[50] Eu, and Yb.[51,52] The corresponding (8s7p6d1f)/[6s5p3d1f] valence basis set for Sc was taken from the literature, whereas the (7s6p5d)/[5s4p3d] valence basis sets for Eu and Yb were augmented by one set of f-functions. The basis sets for C, H, F, and S were either 6–31G* or 6–31+G** [$Yb(SH)_2$ species only]. Frequency calculations were carried out to verify that the geometries were true minima on the potential-energy surface and to obtain the zero-point energy ($E_{ZPE}$). The sum of the electronic energy ($E_e$) and the zero-point energy was used to calculate differences interpreted as reaction enthalpies ($\Delta H_0$) at 0 K. For calibration purposes, test calculations were performed to compute the cation–ring binding energy of $[Sc(C_6H_6)]^+$, which was determined experimentally as $-222 \pm 21$ kJ $mol^{-1}$.[53,54] The results of B3LYP and MP2 calculations with the 6–31+G** basis set fall within the experimental error bars. The binding energy was found to be overestimated by 9–16% using the 6–31G* or 6–311+G** basis sets.

## Acknowledgments

Support of this work by the Fonds der Chemischen Industrie is gratefully acknowledged. The author also wishes to thank Prof. G. Becker for generous support.

[1] M. N. Bochkarev, L. N. Zakharov, G. S. Kalinina, *Organoderivatives of Rare Earth Elements*, Kluwer Academic Press, Dordrecht, **1995**.
[2] F. T. Edelmann, *Angew. Chem.* **1995**, *107*, 2647–2669; *Angew. Chem. Int. Ed. Engl.* **1995**, *34*, 2466–2488.
[3] S. A. Cotton, *Coord. Chem. Rev.* **1997**, *160*, 93–127.
[4] F. Nief, *Coord. Chem. Rev.* **1998**, *178–180*, 13–81.
[5] J. M. Boncella, R. A. Andersen, *Organometallics* **1985**, *4*, 205–206.
[6] P. B. Hitchcock, M. F. Lappert, R. G. Smith, R. A. Bartlett, P. P. Power, *J. Chem. Soc., Chem. Commun.* **1988**, 1007–1009.
[7] P. B. Hitchcock, J. A. K. Howard, M. F. Lappert, S. Prashar, *J. Organomet. Chem.* **1992**, *437*, 177–189.
[8] W. J. Evans, R. Anwander, J. W. Ziller, *Inorg. Chem.* **1995**, *34*, 5927–5930.
[9] M. Westerhausen, M. Hartmann, W. Schwarz, *Inorg. Chim. Acta* **1998**, *269*, 91–100.
[10] W. T. Klooster, R. S. Lu, R. Anwander, W. J. Evans, T. F. Koetzle, R. Bau, *Angew. Chem.* **1998**, *110*, 1326–1329; *Angew. Chem. Int. Ed.* **1998**, *37*, 1268–1270.
[11] W. T. Klooster, L. Brammer, C. J. Schaverien, P. H. M. Budzelaar, *J. Am. Chem. Soc.* **1999**, *121*, 1381–1382.
[12] G. B. Deacon, Q. Shen, *J. Organomet. Chem.* **1996**, *506*, 1–17.
[13] M. Niemeyer, S.-O. Hauber, *Z. Anorg. Allg. Chem.* **1999**, *625*, 137–140.
[14] G. B. Deacon, C. M. Forsyth, P. C. Junk, B. W. Skelton, A. H. White, *Chem. Eur. J.* **1999**, *5*, 1452–1459.
[15] G. Heckmann, M. Niemeyer, *J. Am. Chem. Soc.* **2000**, *122*, 4227–4228.
[16] B. Twamley, S. T. Haubrich, P. P. Power, *Adv. Organomet. Chem.* **1999**, *44*, 1–65.
[17] G. B. Deacon, G. D. Fallon, C. M. Forsyth, H. Schumann, R. Weimann, *Chem. Ber./Recueil* **1997**, *130*, 409–415.
[18] D. F. Evans, G. V. Fazakerley, R. F. Phillips, *J. Chem. Soc. A* **1971**, 1931–1934.
[19] C. Eaborn, P. B. Hitchcock, K. Izod, Z.-R. Lu, J. D. Smith, *Organometallics* **1996**, *15*, 4783–4790.
[20] C. Eaborn, P. B. Hitchcock, K. Izod, J. D. Smith, *J. Am. Chem. Soc.* **1994**, *116*, 12071–12072.
[21] M. Niemeyer, *Z. Anorg. Allg. Chem.* **2000**, *626*, 1027–1029.
[22] The precipitated $YbI_2(THF)_4$ was identified by $^{171}Yb$ NMR and UV/Vis spectroscopy. The latter method also showed the absence of $Yb^{III}$ impurities.
[23] F. T. Edelmann, *Lanthanides and Actinides* in *Synthetic Methods of Organometallic and Inorganic Chemistry (Hermann/Brauer)* (Ed.: W. A. Hermann), Georg Thieme Verlag, Stuttgart, **1997**.
[24] M. Niemeyer, unpublished results.
[25] D. J. Duncalf, P. B. Hitchcock, G. A. Lawless, *Chem. Commun.* **1996**, 269–271.
[26] G. B. Deacon, S. C. Harris, G. Meyer, D. Stellfeldt, D. L. Wilkinson, G. Zelesny, *J. Organomet. Chem.* **1996**, *525*, 247–254.
[27] A search of the CCDC database (Vers. April 2000) for $Yb^{III}$–O(THF) distances with a six-coordinate metal center gave 23 hits in the range 225.5 to 240.9 pm (av. 231.9 pm). A search for the *trans*-O(THF)–$Yb^{III}$–O(THF) fragment resulted in seven hits with an average distance of 226.9 pm.
[28] L. N. Bochkarev, T. A. Zheleznova, A. V. Safronova, M. S. Drozdov, S. F. Zhiltsov, L. N. Zakharov, G. K. Fukin, S. Y. Khorshev, *Russ. Chem. Bull.* **1998**, *47*, 165–168.
[29] G. B. Deacon, T. C. Feng, B. W. Skelton, A. H. White, *Aust. J. Chem.* **1995**, 741–756.
[30] F. G. N. Cloke, *Chem. Soc. Rev.* **1993**, 17–24.

[31] F. G. N. Cloke, K. Khan, R. N. Perutz, *J. Chem. Soc., Chem. Commun.* **1991**, *48*, 1372−1373.
[32] B. Cetinkaya, P. B. Hitchcock, M. F. Lappert, R. G. Smith, *J. Chem. Soc., Chem. Commun.* **1992**, 932−934.
[33] J. R. van den Hende, P. B. Hitchcock, S. A. Holmes, M. F. Lappert, W. P. Leung, T. C. W. Mak, S. Prashar, *J. Chem. Soc., Dalton Trans.* **1995**, 1427−1433.
[34] J. M. Keates, G. A. Lawless, *$^{171}$Yb NMR Spectroscopy* in *Advanced Applications of NMR to Organometallic Chemistry* (Eds.: M. Gielen, R. Willem, B. Wrackmeyer), Wiley, Chichester, **1996**, chapter 12.
[35] W. G. van der Sluys, C. J. Burns, J. C. Huffman, A. P. Sattelberger, *J. Am. Chem. Soc.* **1988**, *110*, 5924−5925.
[36] D. M. Barnhart, D. L. Clark, J. C. Gordon, J. C. Huffman, R. L. Vincent, J. G. Watkin, B. D. Zwick, *Inorg. Chem.* **1994**, *33*, 3487−3497.
[37] R. J. Butcher, D. L. Clark, S. K. Grumbine, R. L. Vincent-Hollis, B. L. Scott, J. G. Watkin, *Inorg. Chem.* **1995**, *34*, 5468−5476.
[38] W. A. King, S. Di Bella, G. Lanza, K. Khan, D. J. Duncalf, F. G. N. Cloke, I. L. Fragala, T. J. Marks, *J. Am. Chem. Soc.* **1996**, *118*, 627−635.
[39] G. Hong, F. Schautz, M. Dolg, *J. Am. Chem. Soc.* **1999**, *121*, 1502−1512.
[40] M. Dolg, H. Stoll, H. Preuss, *J. Mol. Struct. (Theochem)* **1991**, *235*, 67−79.
[41] M. Kaupp, P. v. R. Schleyer, M. Dolg, H. Stoll, *J. Am. Chem. Soc.* **1992**, *114*, 8202−8208.
[42] M. Kaupp, P. v. R. Schleyer, *J. Am. Chem. Soc.* **1992**, *114*, 491−497.
[43] R. Blom, K. Faegri, Jr., H. V. Volden, *Organometallics* **1990**, *9*, 372−379.
[44] M. Niemeyer, P. P. Power, *Inorg. Chem.* **1996**, *35*, 7264−7272.
[45] H. Hope, *Handling of Reactive Compounds for X-ray Structure Analysis* in *Experimental Organometallic Chemistry: A Practicum in Synthesis and Characterization* (Eds.: A. L. Wayda, M. Y. Darensbourg), American Chemical Society, Washington DC, **1987**, chapter 10.
[46] *SHELXTL PC 5.03*, Siemens Analytical X-ray Instruments Inc., Madison, WI, **1994**.
[47] G. M. Sheldrick, *Program for Crystal Structure Solution and Refinement*, Universität Göttingen, **1997**.
[48] S. Parkin, B. Moezzi, H. Hope, *J. Appl. Crystallogr.* **1995**, *28*, 53−56.
[49] M. J. Frisch, G. W. Trucks, H. B. Schlegel, G. E. Scuseria, M. A. Robb, J. R. Cheeseman, V. G. Zakrzewski, J. A. Montgomery, Jr., R. E. Stratmann, J. C. Burant, S. Dapprich, J. M. Millam, A. D. Daniels, K. N. Kudin, M. C. Strain, O. Farkas, J. Tomasi, V. Barone, M. Cossi, R. Cammi, B. Mennucci, C. Pomelli, C. Adamo, S. Clifford, J. Ochterski, G. A. Petersson, P. Y. Ayala, Q. Cui, K. Morokuma, D. K. Malick, A. D. Rabuck, K. Raghavachari, J. B. Foresman, J. Cioslowski, J. V. Ortiz, A. G. Baboul, B. B. Stefanov, G. Liu, A. Liashenko, P. Piskorz, I. Komaromi, R. Gomperts, R. L. Martin, D. J. Fox, T. Keith, M. A. Al-Laham, C. Y. Peng, A. Nanayakkara, C. Gonzalez, M. Challacombe, P. M. W. Gill, B. Johnson, W. Chen, M. W. Wong, J. L. Andres, C. Gonzalez, M. Head-Gordon, E. S. Replogle, J. A. Pople, *Gaussian 98, Rev. A.7*, Gaussian, Inc., Pittsburgh PA, **1998**.
[50] M. Dolg, U. Wedig, H. Stoll, H. Preuss, *J. Chem. Phys.* **1987**, *86*, 866−872.
[51] M. Dolg, H. Stoll, A. Savin, H. Preuss, *Theor. Chim. Acta* **1989**, *75*, 173−194.
[52] M. Dolg, H. Stoll, H. Preuss, *Theor. Chim. Acta* **1993**, *85*, 441−450.
[53] L. M. Lech, B. S. Freiser, *Organometallics* **1988**, *7*, 1948−1957.
[54] C. W. Bauschlicher Jr., H. Partridge, S. R. Langhoff, *J. Phys. Chem.* **1992**, *96*, 3273−3278.
[55] K. Mashima, Y. Nakayama, H. Fukumoto, N. Kanehisa, Y. Kai, A. Nakamura, *J. Chem. Soc., Chem. Commun.* **1994**, 2523−2524.
[56] M. Berardini, J. G. Brennan, *Inorg. Chem.* **1995**, *34*, 6179−6185.
[57] M. Brewer, D. Khasnis, M. Buretea, M. Berardini, T. J. Emge, J. G. Brennan, *Inorg. Chem.* **1994**, *33*, 2743−2747.
[58] F. Nief, L. Ricard, *J. Chem. Soc., Chem. Commun.* **1994**, 2723−2724.
[59] M. Berardini, J. Lee, D. Freedman, J. Lee, T. J. Emge, J. G. Brennan, *Inorg. Chem.* **1997**, *36*, 5772−5776.
[60] H. C. Aspinall, S. A. Cunningham, P. Maestro, P. Macaudiere, *Inorg. Chem.* **1998**, *37*, 5396−5398.
[61] H. Liang, Q. Shen, S. Jin, Y. Lin, *J. Chem. Soc., Chem. Commun.* **1992**, 480−481.
[62] H. Liang, Q. Shen, J. Guan, Y. Lin, *J. Organomet. Chem.* **1994**, *474*, 113−116.
[63] G. B. Deacon, S. Nickel, P. MacKinnon, E. R. T. Tiekink, *Aust. J. Chem.* **1990**, *43*, 1245−1257.

Received October 17, 2000
[I00395]